Bioorganic Chemistry 86 (2019) 473–481

Contents lists available at ScienceDirect

Bioorganic Chemistry

journal homepage: www.elsevier.com/locate/bioorg

Investigation on the effect of alkyl chain linked mono-thioureas as Jack bean urease inhibitors, SAR, pharmacokinetics ADMET parameters and molecular docking studies

Fayaz Ali Larik[a,*], Muhammad Faisal[a,*], Aamer Saeed[a,*], Pervaiz Ali Channar[a], Jan Korabecny[b], Farukh Jabeen[e], Ihsan Ali Mahar[a], Mehar Ali Kazi[d], Qamar Abbas[g], Ghulam Murtaza[a], Gul Shahzada Khan[f], Mubashir Hassan[c], Sung-Yum Seo[c]

[a] Department of Chemistry, Quaid-I-Azam University, Islamabad 45320, Pakistan
[b] Biomedical Research Centre, University Hospital Hradec Kralove, Sokolska 581, 500 05 Hradec Kralove, Czech Republic
[c] Department of Biological Sciences, College of Natural Sciences, Kongju National University, 56 Gongjudehak-Ro, Gongju, Chungnam 314-701, Republic of Korea
[d] Institute of biochemistry, University of Sindh, Jamshoro 76080, Pakistan
[e] Cardiovascular and Metabolic Research Unit, Laurentian University, 935 Ramsey Lake Road, Sudbury, ON P3E 2C6, Canada
[f] Department of Chemistry, Abdul Wali Khan University, Mardan, Khybder Pakhtunkhwa, Pakistan
[g] Department of Physiology, University of Sindh, Jamshoro 76080, Pakistan

ARTICLE INFO

Keywords:
Lipinski's rules
Acyl thioureas
Kinetic mechanism
Antioxidant
Molecular modeling
Jack bean urease
Urease

ABSTRACT

The increasing resistance of pathogens to common antibiotics, as well as the need to control urease activity to improve the yield of soil nitrogen fertilization in agricultural applications, has stimulated the development of novel classes of molecules that target urease as an enzyme. In this context, the newly developed compounds on the basis of 1-heptanoyl-3-arylthiourea family were evaluated for Jack bean urease enzyme inhibition activity to validate their role as potent inhibitors of this enzyme. 1-Heptanoyl-3-arylthioureas were obtained in excellent yield and characterized through spectral and elemental analysis. All the compounds displayed remarkable potency against urease inhibition as compared to thiourea standard. It was found that novel compounds fulfill the criteria of drug-likeness by obeying Lipinski's rule of five. Particularly compound **4a** and **4c** can serve as lead molecules in 4D (drug designing discovery and development). Kinetic mechanism and molecular docking studies also carried out to delineate the mode of inhibition and binding affinity of the molecules.

1. Introduction

The enzyme urease (urea amidohydrolase; E.C.3.5.1.5) has a storied history and constantly been exploited by medicinal chemist to develop potent and efficient inhibitors of this enzyme [1]. Urease helps in the hydrolysis of urea, an essential fertilizer for soil, by cleaving urea into ammonia and carbon dioxide. Both the ammonia gas and carbon dioxide are not ecofriendly and can cause catastrophic alterations in the crop production [2]. In addition to this, urease provide an aid to *Heliobacter pylori* (*H. Pylori*) to survive in the stomach. Urease test is a rapid diagnostic test for diagnosis of *H. pylori* infection in the human stomach. Settlement by *H. pylori* can stimulate pathogenesis of many human health conditions vis-à-vis pyelonephritis, heptatic coma, peptic ulceration and urinary catheter encrustation [3].

Urease inhibitors can serve as key precursors to prevent stomach and urinary related disorders in human beings and also to prevent soil from damage caused by the excess of ammonia release from urea during hydrolysis [4]. Urease inhibitors have broadly classified mainly into two categories (i) active site directed (substrate-like), and (ii) mechanism-based directed [5]. Several classes of compounds are reported to show significant inhibition against urease enzyme, most commonly hydroxamic acids (HXAs) [6], phosphorodiamidates (PPDs) [7], imidazoles [8], phosphazene [9], thioureas [10] and related compounds [11].

Acyl thiourea family is versatile class of organic compounds representing basic scaffold in medicinal and synthetic chemistry [12]. Acyl thioureas motif has been the valuable synthon in the synthesis of wide variety of heterocyclic compounds [13–15]. In addition to being important in synthetic chemistry, these show broad spectrum of biological activities such as antioxidant, antifungal, antimicrobial,

* Corresponding authors. Tel.: +92 51 9064 2128; fax: +92 51 9064 2241 (A. Saeed).
E-mail addresses: fayazali@chem.qau.edu.pk (F.A. Larik), mfaisal4646@gmail.com (M. Faisal), aamersaeed@yahoo.com (A. Saeed).

https://doi.org/10.1016/j.bioorg.2019.02.011
Received 13 December 2018; Received in revised form 30 January 2019; Accepted 3 February 2019
Available online 08 February 2019
0045-2068/

antiviral, anti-cancer, anti-tuberculosis, antibacterial, herbicidal and insecticidal [16].

The structure-activity relationship [17] and literature data of thioureas-derived *N*-bridged alkyl compounds [18–20] reveal that these compounds have wide bioactive spectrum. In view of these particulars and by taking into account to extend alkyl chain up to six carbons, we designed and synthesized acyl thioureas as Jack bean urease inhibitors. The inhibition ability for these new low-molecular weight thioureas were in micromolar range. The results of our work would serve as templates for the designing potent drugs against Jack bean urease enzyme.

2. Experimental

2.1. Methods and materials

^{1}H NMR and ^{13}C NMR spectra were recorder on a Brucker AM-300 spectrophotometer and chemical shifts of ^{1}H NMR and ^{13}C NMR are reported in parts per million (ppm). Internal standard TMS; the splitting of proton resonances in the reported ^{1}H NMR spectra are defined as s = singlet, d = doublet, q = quartet, dd = doublet of doublets, se = septet and m = complex pattern. The melting point was determined on Staurt SMP3 melting point apparatus and is uncorrected. FTIR spectra were recorded using Shimadzu IR 460 spectrophotometer by Attenuated Total Reflectance (ATR) method. The elemental analysis was performed on LECO-932 CHNS analyzer.

For organic chemistry part, all experiments were performed under the specified conditions of temperature. Solvents were distilled from the appropriate drying agents and degassed before use. All solvents were purified by distillation, dried, saturated with nitrogen and stored over molecular sieves 4 Å. Heptanoic acid, potassium thiocyanate, thionyl chloride, 2,4-dinitroaniline, 2,3-dichloroaniline, 4-bromoaniline, 4-chloroaniline, 3-nitroaniline, 2-chloroaniline, 2,4,6-trimethylaniline, 4-nitroaniline, and 2-bromo-2-flouroaniline were purchased from Sigma-Aldrich, Australia and used as received.

2.2. Experimental data

2.2.1. 1-Heptanoyl-3-(2, 4-nitrophenyl) thiourea (4a)

Yellow solid; R_f (*n*-hexane: ethylacetate 1:1); 0.49; m.p: 198 °C; IR (neat, cm^{-1}): 3234 (N—H), 1670 (C═O), 1549 (NH), 1261 (C═S). ^{1}H NMR (DMSO-d_6), 300 MHz): 12.25 (s, 1H, NH), 11.63 (s, 1H, NH), 7.83 (d, 1H, *J* = 7.12 Hz, Ar-H), 7.53 (d, 1H, *J* = 7.52 Hz, Ar-H), 7.52 (d, 1H, *J* = 7.52 Hz, Ar-H), 2.82 (t, 2H, *J* = 3.3 Hz), 2.11 (quint, 2H, *J* = 2.2 Hz), 1.93 (quint, 2H), 1.32 (quint, 2H), 0.92 (sex, 2H), 0.86 (t, 3H, *J* = 1.1 Hz);^{13}C NMR (DMSO-d_6); 75.5 MHz): 180.6, 175.4, 157.9, 152.1, 135.2, 129.7, 120.7, 118.2, 36.5, 31.5, 28.5, 25.7, 22.7, 15.1, Anal. Calcd. For $C_{14}H_{18}N_4O_5S$, C, 47.44; H, 5.12; N, 15.81; S 9.04; Found: C, 47.33, H, 4.99; N, 15.73; S, 8.97.

2.2.2. 1-Heptanoyl-3-(2, 3-dichlorophenyl) thiourea (4b)

Yellow solid; R_f (*n*-hexane: ethylacetate 1:1); 0.49; m.p: 198 °C; IR (neat, cm^{-1}): 3234 (m, N—H), 1670 (C═O), 1549 (NH), 1261 (C═S). ^{1}H NMR (DMSO-d_6), 300 MHz): 12.25 (s, 1H, NH), 11.63 (s, 1H, NH), 7.73 (d, 1H, *J* = 7.12 Hz, Ar-H), 7.46 (d, 1H, *J* = 7.52 Hz, Ar-H), 7.36 (d, 1H, *J* = 7.52, Ar-H), 2.91 (t, 2H, *J* = 3 Hz), 2.14 (quint, 2H, *J* = 2 Hz), 1.95 (quint, 2H), 1.34 (quint, 2H), 1.02 (sex, 2H), 0.91 (t, 3H, *J* = 1 Hz); ^{13}C NMR (DMSO-d_6); 75.5 MHz): 179.6, 173.4, 154.19, 140.1, 135.2, 131.7, 125.7, 122.5, 37.3, 32.4, 27.4, 26.4, 23.5, 14.7, Anal. Calcd. For $C_{14}H_{18}Cl_2N_2OS$, C, 50.44; H, 5.44; N, 8.41; S 9.64; Found: C, 50.34, H, 5.32; N, 8.23; S, 9.51.

2.2.3. 1-Heptanoyl-3-(4-bromophenyl) thiourea (4c)

Yellow solid; R_f (*n*-hexane:ethylacetate 1:1); 0.51; m.p: 187 °C; IR (neat, cm^{-1}): 3229 (m, N—H), 1685 (C═O), 1540 (N—H), 1279 (C═S). ^{1}H NMR (DMSO- d_6), 300 MHz): 12.65 (s, 1H, NH), 12.03 (s, 1H, NH), 7.63 (dd, 1H, *J* = 6.3 Hz, *J* = 5.6 Hz, Ar-H), 7.56 (dd, 1H, *J* = 7.1 Hz, *J* = 5.3 Hz Ar-H), 2.42 (t, 2H, *J* = 3 Hz), 2.85 (t, 2H, *J* = 3 Hz), 2.15 (quint, 2H, *J* = 2 Hz), 1.86 (quint, 2H), 1.51 (quint, 2H), 1.19 (sex, 2H), 0.96 (t, 3H, *J* = 1 Hz); ^{13}C NMR (DMSO-d_6); 75.5 MHz): 181.6, 174.4, 148.9, 142.3, 135.4, 130.5, 38.2, 32.3, 27.3, 24.6, 21.5, 16.2, Anal. Calcd. For $C_{14}H_{19}BrN_2OS$, C, 48.96; H, 5.45; N, 8.57; S 9.35; Found: C, 48.69; H, 5.35; N, 8.45; S, 9.24.

2.2.4. 1-Heptanoyl-3-(3-nitrophenyl) thiourea (4d)

Yellow solid; Rf (*n*-hexane: ethylacetate 1:1); 0.53; m.p: 170 °C; IR (neat, cm^{-1}): 3229 (N—H), 1670 (C═O), 1543 (NH), 1260 (C═S). ^{1}H NMR (DMSO-d_6), 300 MHz): 12.22 (s, 1H, NH), 11.26 (s, 1H, NH), 7.69 (d, 1H, *J* = 7.10, Ar-H), 7.56 (d, 1H, *J* = 7.61 Hz, Ar-H), 7.42 (d, 1H, *J* = 7.10 Hz, Ar-H), 7.26 (d, 1H, *J* = 7.61 Hz, Ar-H), 2.91 (t, 2H, *J* = 3 Hz), 2.15 (quint, 2H, *J* = 2 Hz), 1.85 (quint, 2H), 1.38 (quint, 2H), 1.12 (sex, 2H), 0.98 (t, 3H, *J* = 1 Hz);^{13}C NMR (DMSO-d_6); 75.5 MHz): 179.6, 170.4, 152.1, 139.2, 132.5, 129.6, 124.7, 121.5, 36.5, 31.5, 28.5, 25.7, 22.7, 15.1, Anal. Calcd. For $C_{14}H_{19}N_3O_3S$, C, 54.34; H, 6.18; N, 13.57; S 10.35; Found: C, 54.22; H, 599; N, 13.43; S, 10.24.

2.2.5. 1-Heptanoyl-3-(2-chlorophenyl) thiourea (4e)

Light yellow solid; Rf (*n*-hexane: ethyl acetate 1:1); 0.56; m.p: 195 °C; IR (neat, cm^{-1}): 3219 (N—H), 1680 (C═O), 1534 (N—H), 1268 (v C═S). ^{1}H NMR (DMSO-d_6), 300 MHz): 12.65 (s, 1H, NH), 12.03 (s, 1H, NH), 7.41 (d, 1H, *J* = 6.3 Hz, Ar-H), 7.35 (d, 1H, *J* = 5.7 Hz, Ar-H), 7.25 (d, 1H, *J* = 4.7 Hz, Ar-H), 6.99 (d, 1H, *J* = 4.7 Hz, Ar-H), 2.78 (t, 2H, *J* = 3 Hz), 2.11 (quint, 2H, *J* = 2 Hz), 1.93 (quint, 2H), 1.32 (quint, 2H), 0.92 (sex, 2H), 0.86 (t, 3H, *J* = 1 Hz); ^{13}C NMR (DMSO-d_6);75.5 MHz): 179.6, 170.4, 142.19, 137.2, 133.5, 128.6, 125.3, 123.7, 35.4, 32.3, 29.4, 24.6, 21.5, 13.5, Anal. Calcd. For $C_{14}H_{19}ClN_2OS$, C, 56.26; H, 6.42; N, 9.38; S 10.74; Found: C, 56.15; H, 6.29; N, 9.28; S, 10.63.

2.2.6. 1-Heptanoyl-3-(2,4,6-trimethylphenyl) thiourea (4f)

Light yellow solid; Rf (*n*-hexane: ethyl acetate 1:1); 0.56; m.p: 195 °C; IR (neat, cm^{-1}): 3219 (N—H), 1680 (C═O), 1534 (N—H), 1268 (C═S). ^{1}H NMR (DMSO-d_6), 300 MHz): 12.65 (s, 1H, NH), 12.03 (s, 1H, NH), 7.48 (d, 1H, *J* = 4.3 Hz, Ar-H), 7.28 (d, 1H, *J* = 3.3 Hz, Ar-H), 2.78 (t, 2H, *J* = 3 Hz), 2.15 (quint, 2H, *J* = 2 Hz), 1.85 (quint, 2H), 1.35 (quint, 2H), 1.08 (sex, 2H), 0.99 (t, 3H, *J* = 1 Hz);^{13}C NMR (DMSO-d_6);75.5 MHz): 179.6, 170.4, 145.16, 134.5, 127.4, 122.8, 37.1, 29.4, 24.3, 21.7, 18.7, 12.5, Anal. Calcd. For $C_{17}H_{26}N_2OS$, C, 66.61; H, 8.54; N, 9.15; S 10.45; Found: C, 66.48; H, 8.39; N, 9.02; S, 10.34.

2.2.7. 1-Heptanoyl-3-(4-nitrophenyl) thiourea (4 g)

Yellow solid; Rf (*n*-hexane:ethylacetate 1:1); 0.53; m.p: 160 °C; IR (neat, cm^{-1}): 3229 (m, N—H), 1685 (C═O), 1540 (N—H), 1279 (C═S). ^{1}H NMR (DMSO- d_6), 300 MHz): 11.61 (s, 1H, NH), 11.43 (s, 1H, NH), 7.67 (dd, 1H, *J* = 5.3 Hz, *J* = 4.6 Hz, Ar-H), 7.50 (dd, 1H, *J* = 7.2 Hz, *J* = 4.3 Hz Ar-H), 2.51 (t, 2H, *J* = 3 Hz), 2.81 (t, 2H, *J* = 3 Hz), 2.17 (quint, 2H, *J* = 2 Hz), 1.88 (quint, 2H), 1.41 (quint, 2H), 1.13 (sex, 2H), 1.06 (t, 3H, *J* = 1 Hz); ^{13}C NMR (DMSO-d_6); 75.5 MHz): 182.5, 173.7, 145.4, 141.3, 134.6, 129.4, 34.5, 31.5, 26.5, 23.8, 20.9, 17.4, Anal. Calcd. For $C_{14}H_{19}BrN_2OS$, C, 48.96; H, 5.45; N, 8.57; S 9.35; Found: C, 48.69; H, 5.35; N, 8.45; S, 9.24.

2.2.8. 1-Heptanoyl-3-(4-bromo-2-flourophenyl) thiourea (4 h)

White solid; R_f (*n*-hexane: ethylacetate 1:1); 0.58; m.p: 201 °C; IR (neat, cm^{-1}): 3230 (m, N—H), 1676 (C═O), 1547 (N—H), 1269 (C═S). ^{1}H NMR (DMSO-d_6), 300 MHz): 12.11 (s, 1H, NH), 11.68(s, 1H, NH), 7.93 (d, 1H, *J* = 7.10 Hz, Ar-H), 7.56 (d, 1H, *J* = 7.61 Hz, Ar-H), 2.85 (t, 2H, *J* = 3 Hz), 2.18 (quint, 2H, *J* = 2 Hz), 1.83 (quint, 2H), 1.22 (quint, 2H), 1.12 (sex, 2H), 0.89 (t, 3H, *J* = 1 Hz); ^{13}C NMR (DMSO-d_6); 75.5 MHz): 179.6, 170.4, 152.19, 142.5, 135.8, 133.1, 128.5, 121.8, 34.8, 32.8, 26.3, 24.8, 22.7, 12.4, Anal. Calcd. For $C_{14}H_{18}BrFN_2OS$, C,

46.53; H, 5.04; N, 7.76; S 8.84; Found: C, 46.41; H, 4.96; N, 7.59; S, 8.74.

2.2.9. 1-Heptanoyl-3-(2,6-dibromo-4-flourophenyl) thiourea (4i)

Light yellow solid; Rf (*n*-hexane: ethyl acetate 1:1); 0.56; m.p: 195 °C; IR (neat, cm^{-1}): 3219 (N—H), 1680 (C═O), 1534 (N—H), 1268 (C═S). ^{1}H NMR (DMSO-d_6), 300 MHz): 12.65 (s, 1H, NH), 12.03 (s, 1H, NH), 7.48 (d, 1H, J = 4.3 Hz, Ar-H), 7.28 (d, 1H, J = 3.3, Ar-H), 2.78 (t, 2H, J = 3 Hz), 2.15 (quint, 2H, J = 2 Hz), 1.85 (quint, 2H), 1.35 (quint, 2H), 1.08 (sex, 2H), 0.99 (t, 3H, J = 1 Hz);^{13}C NMR (DMSO-d_6);75.5 MHz): 179.6, 170.4, 145.16, 134.5, 127.4, 122.8, 37.1, 29.4, 24.3, 21.7, 18.7, 12.5, Anal. Calcd. For $C_{14}H_{17}Br_2FN_2OS$, C, 38.20; H, 3.89; N, 6.35; S 7.29; Found: C, 38.12; H, 3.39; N, 9.02; S, 10.34.

2.2.10. 1-Heptanoyl-3-benzylthiourea (4j)

White solid; R_f (*n*-hexane: ethylacetate 1:1); 0.58; m.p: 221 °C; IR (neat, cm^{-1}): 3230 (s, N—H), 1676 (C═O), 1547 (v, N—H), 1250 (C═S). ^{1}H NMR (DMSO-d_6), 300 MHz): 12.11 (s, 1H, NH), 11.68 (s, 1H, NH), 7.93 (dd, 2H, J = 5.1 Hz, J = 3.6 Hz, Ar-H), 7.56 (dd, 2H, J = 7.61 Hz Ar-H), 7.23 (d, 1H, J = 5.3 Hz), 2.82 (t, 2H, J = 3 Hz), 2.11 (quint, 2H, J = 2 Hz), 1.93 (quint, 2H), 1.32 (quint, 2H), 0.92 (sex, 2H), 0.86 (t, 3H, J = 1 Hz);^{13}C NMR (DMSO-d_6); 75.5 MHz): 179.6, 170.4, 143.19, 135.2, 133.7, 132.3, 36.7, 31.5, 28.5, 25.7, 22.7, 15.1, Anal. Calcd. For $C_{15}H_{22}N_2OS$, C, 64.69; H, 7.94; N, 10.06; S 11.51; Found: C, 64.57; H, 7.86; N, 9.92; S, 11.41.

2.3. Biological activity, kinetics and molecular docking methods and procedure

2.3.1. Urease inhibition assay

The Jack bean urease activity was determined by measuring amount of ammonia produced with indophenols method described by Weatherburn [21]. The reaction mixtures, comprising 20 μL of enzyme (Jack bean urease, 5 U/mL) and 20 μL of compounds in 50 μL buffer (100 mM urea, 0.01 M K_2HPO_4, 1 mM EDTA and 0.01 M LiCl, pH 8.2), were incubated for 30 min at 37 °C in 96-well plate. Briefly, 50 μL each of phenol reagents (1%, w/v phenol and 0.005%, w/v sodium nitroprusside) and 50 μL of alkali reagent (0.5%, w/v NaOH and 0.1% Sodium hypochlorite NaOCl) were added to each well. The absorbance at 625 nm was measured after 10 min, using a microplate reader (OPTI$_{Max}$, Tunable). All reactions were performed in triplicate. The urease inhibition activities were calculated according to the following formula:

$$\text{Urease inhibition activity}(\%) = (OD_{control} - -OD_{sample} \times 100)/OD_{control}$$

where $OD_{control}$ and OD_{sample} represents the optical densities in the absence and presence of sample, respectively [11]. Thiourea was used as the standard inhibitor for urease.

2.3.2. Kinetic study

Kinetic analysis was carried out to determine the mode of inhibition. Two inhibitors (**4a** and **4c**) were selected on the basis of most potent IC_{50} values. Kinetics were carried out by varying the concentration of urea in the presence of different concentrations of compound H1 (0.0, 0.0195, 0.039, 0.078 and 0.312), compound **4c** (0.00, 0.02, 0.04, and 0.08 μM). Briefly the urea concentration was changed from 100, 50, 25, 12.5, 6.25, 3.12 mM for urease kinetics studies and remaining procedure was same for all kinetic studies as describes in urease inhibition assay protocol. Maximal initial velocities were determined from initial linear portion of absorbances up to 10 min after addition of enzyme at per minute's interval. The inhibition type on the enzyme was assayed by Lineweaver-Burk plot of inverse of velocities (1/V) versus inverse of substrate concentration 1/[S] mM^{-1}. The EI dissociation constant Ki was determined by secondary plot of 1/V versus inhibitor concentration. Urease activity was determined by measuring ammonia production using the indophenol method as reported previously [22]. The results (change in absorbance per min) were processed by using SoftMaxPro.

2.3.3. Free radical scavenging assay

Radical scavenging activity was determined by modifying already reported method by 2,2-diphenyl-1 picrylhydrazyl (DPPH) assay [22]. The assay solution consisted of 100 μL of DPPH (150 μM), 20 μL of increasing concentration of test compounds and the volume was adjusted to 200 μL in each well with DMSO. The reaction mixture was then incubated for 30 min at room temperature. Ascorbic acid (Vitamin C) was used as a reference inhibitor. The assay measurements were carried out by using a micro plate reader (OPTI $_{Max}$, Tunable) at 517 nm. The reaction rates were compared and the percent inhibition caused by the presence of tested inhibitors was calculated [23]. Each concentration was analyzed in three independent experiments run in triplicate.

2.4. Computational methodology

2.4.1. Retrieval of Jack bean urease structure from PDB

The Jack bean urease structure was retrieved from Protein Data Bank (PDB) (www.rcsb.org) with PDBID 4H9M. The selected crystal structure of urease was minimized by using UCSF Chimera 1.10.1 tool [24]. Furthermore, the stereo-chemical properties of urease structure and Ramachandran plot and values were generated by Molprobity server and Protparam, respectively [25]. The Discovery Studio 4.1 Client was used to generate the hydrophobicity graph of target protein [26]. The protein architecture and statistical percentage values of receptor proteins helices, beta-sheets, coils and turn were predicted from online server VADAR 1.8 [27].

2.4.2. Molecular docking simulation

The synthesized chemical structures (**4a-j**) were sketched in ACD/ChemSketch tool and minimized by UCSF Chimera 1.10.1 tool [28]. The molecular docking experiments were performed using PyRx docking through VINA wizard. The grid box center values were adjusted as for X = 10.48, Y = −55.22 and Z = −26.48), respectively. While, the size parameters values (X = 66.60, Y = 60.08, and Z = 56.84) were also focused to get the better conformational binding poses. The default exhaustiveness value was used to maximize the binding conformational analysis. All the synthesized ligands were docked separately against urease receptor. The Autodock VINA scoring function equation is mentioned supplementary data. The predicted docked complexes were evaluated on the basis of lowest binding energy (Kcal/mol) values and structure activity relationship (SAR) analyses. The three dimensional (3D) graphical depictions of all the docked complexes were accomplished by Discovery Studio (2.1.0).

3. Results

3.1. Synthetic chemistry

The designed compounds were synthesized by using heptanoic acid (**1**) as starting material. Heptanoic acid was treated with thionyl chloride to convert carboxylic acid functionality into heptanoyl chloride. Next, the acid was treated with easily available potassium thiocyanate in dry acetone to form key reactive intermediate isothiocyanate (**2**) which was not isolated (no isolation required for next step) [23,29]. In last step, substituted aromatic amines were reacted with isothiocyanate to afford 1-heptanoyl-3-arylthioureas in excellent yield (84–90%). The synthesis of new 1-heptanoyl-3-arylthioureas (**4a-4j**) is outlined in the Scheme 1.

3.2. Urease inhibitory activity

The urease enzyme inhibition activity results are summarized in Table 1. All the compounds showed significant potential of inhibition

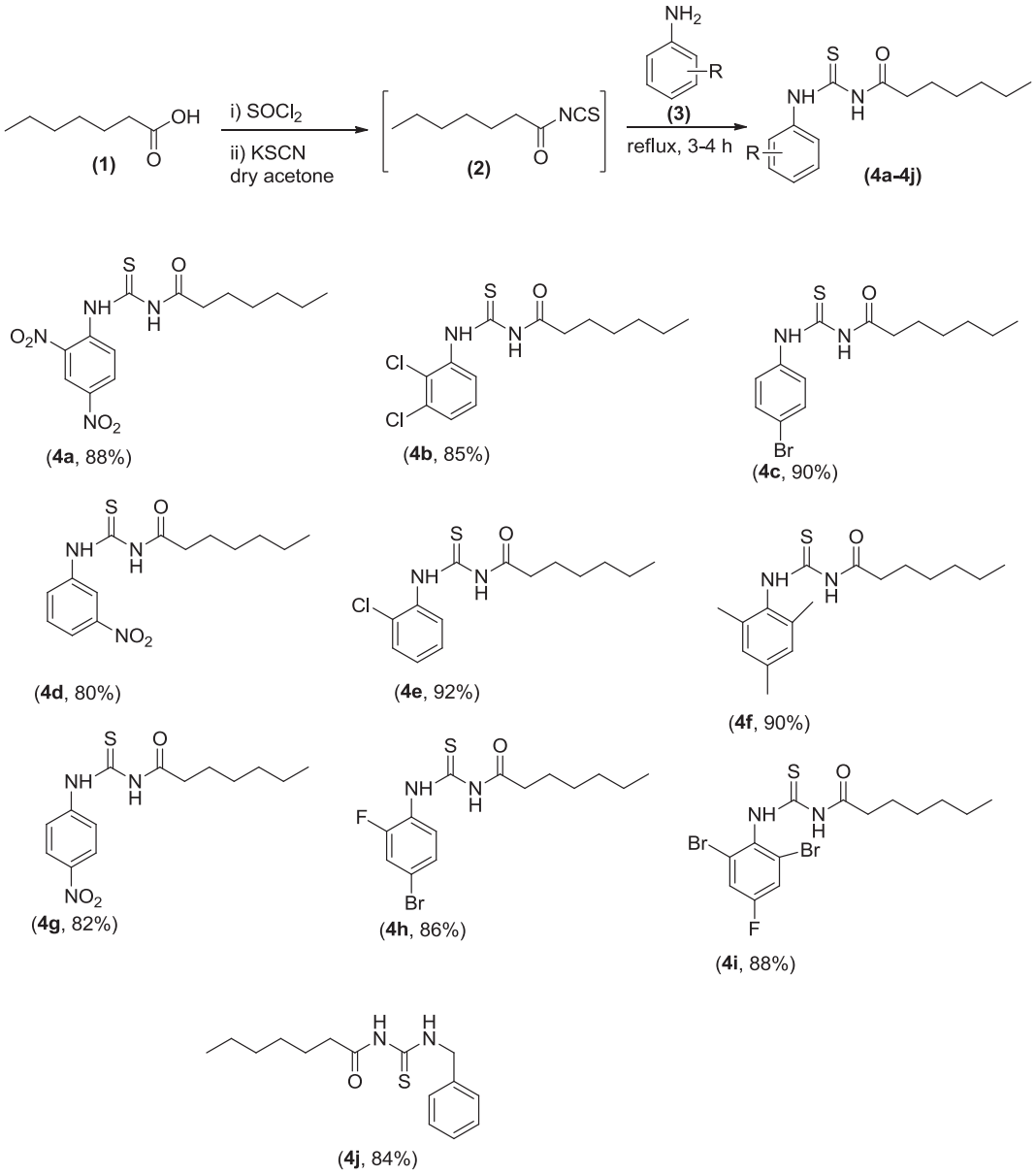

Scheme 1. Synthetic pathway along with the obtained yield of 1-heptanoyl-3-arylthioureas (**4a-4j**).

Table 1
Urease inhibitory activity of 1-Heptanoyl-3-arylthioure derivatives (**4a-4j**).

Compound	Urease(Jack bean) IC_{50} ± SEM (μM)
4a	0.0313 ± 0.0021
4b	0.0445 ± 0.0036
4c	0.0396 ± 0.0038
4d	0.0621 ± 0.0041
4e	0.0644 ± 0.0062
4f	0.1246 ± 0.0091
4g	0.1551 ± 0.021
4h	0.1554 ± 0.024
4i	0.0934 ± 0.0082
4j	0.1112 ± 0.081
Thiourea	18.482 ± 0.461

Values are expressed as mean ± SEM.
SEM = Standard Error of Mean.

against Jack bean urease enzyme with IC_{50} values ranging in micromolar range. Moreover, all the compounds showed higher potential than the thiourea standard. The compound **4a** and **4c** showed significant level of inhibition compared to other derivatives in the series. The compound **4a** bears two nitro groups at *ortho*- and *para*-position which perturbs electron density and further pull apart electronic cloud. Compound **4c** bear halogen atom, bromine at *para* position; hence, due to large atomic size, lipophilic character of the derivative enhances. The structure activity of relationship of the most potent derivatives is depicted in Fig. 1

4. Discussion

4.1. Chemistry

The synthesized compounds were characterized through FT-IR, CHNS analysis, melting point, ^{1}H NMR and ^{13}C NMR spectroscopy. The appearance of peak at 3400–3300 cm^{-1} was assigned to N—H moiety. The characteristic peak for thiocarbonyl appear at 1255–1220 cm^{-1}. The C—H sp^2 stretching for benzene ring appeared at 1500–1400 cm^{-1}. The ^{1}H NMR spectrum also revealed the formation of compounds. The most deshielded signal appeared for N—H at 12–11 ppm. As thioureas contains two distinct N—H groups so these two hydrogens appeared as

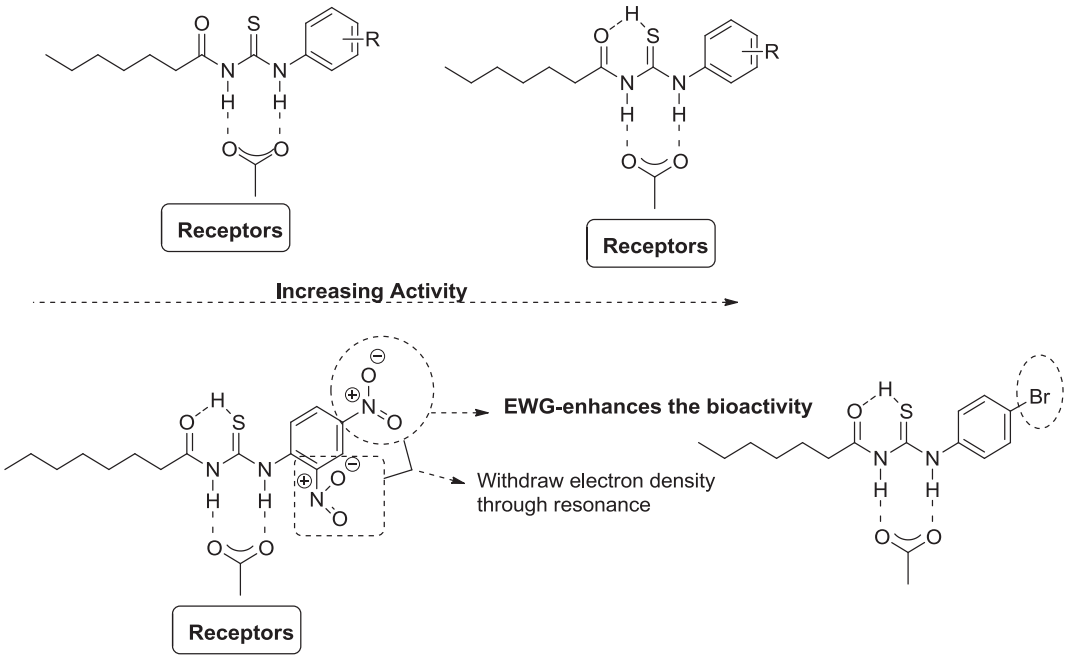

Fig. 1. Structure activity relationship of most potent derivatives **4a** and **4c** derivatives.

distinct singlets. The appearance of signal at 7–8 ppm was attributed to aromatic part. The alkyl part appeared at 2–3 ppm value. The ^{13}C NMR spectroscopy also showed formation of title compounds. The characteristic peak for thiocarbonyl appeared at 180 ppm value while carbonyl appeared at 170 ppm value. The appearance of signals at 140–120 was assigned to aromatic part. The sp^3 carbons appeared at around 30–20 ppm.

4.2. Kinetic study

Based on our results we selected the most potent compounds, namely **4a** and **4c**, to determine their inhibition type and inhibition constant on jack bean urease. The potential of these compounds to inhibit free enzyme and enzyme substrate complex was determined in term of EI and ESI constants respectively. The kinetic studies of the enzyme by the Lineweaver-Burk plot of 1/V versus 1/[S] in the presence of different compounds concentrations gave a series of straight lines (Fig. 2). The results of both **4a** and **4c** showed that compound intersected within the second quadrant. The analysis showed that V_{max} decreased to new increasing doses of inhibitors on the other hand K_m remains the same. This behavior indicates that both compounds inhibit the urease non-competatively to form enzyme inhibitor complex. Secondary plot of slope against the concentration of inhibitors showed enzyme inhibitor dissociation constant (K_i) (Fig. 3)

The kinetic results are presented in the Table 2.

4.3. Structural and physiochemical evaluation of Jack bean urease

Jack bean urease is a class of hydrolase protein which consists of four domains having different numbers of amino acids. Two nickel atoms are also present in the active region of target protein. The overall statistical VADAR analysis showed the protein architecture which contains 27% helices, 31% β sheets and 41% coils. Moreover, Ramachandran plots indicated that 97.5% of residues were present in favored regions which show the precision of phi (φ) and psi (ψ) angles among the coordinates of jack bean urease.

4.4. Chemo-informatics properties and Lipinski's rule of synthesized compounds

The predicted chemo-informatic properties such as molar volume and refractivity, density, polarizability and surface tension were evaluated by computational approaches. Kadam and his colleagues have depicted some standard value for molar refractivity (40 to 130) and molecular weight (160 to 480), respectively [30]. Results show that compounds **4a-j** have better predicted values compared to standard values. Moreover, the Lipinski's rule of five (RO5) results showed that compounds (**4a-j**) possess good HBA, HBD and log*P* values which are significantly justified its drug like behavior [31]. Moreover, their molecular weight of all compounds was also comparable with standard value (< 5000 g/mol). The RO5 justifies that molecules with poor absorption are more likely to have more than 5 HBD, MWT over 500, log*P* over 5 and more than 10 HBA. However there are plenty of examples available for RO5 violation amongst the existing drugs [32]. The overall predicted values for all the compounds are mentioned in Table 3.

4.5. Pharmacokinetic properties of screened compounds

The development of novel candidate molecule requires high attention rate with good pharmacokinetic properties. Most probably the absorption, distribution, metabolism, excretion and toxicity (ADMET) properties assessment were considered as major hallmark to confirm the efficacy of lead molecules. To check the pharmacokinetic behavior of our synthesized compounds (**4a-j**), pkCSM online server was employed to predict the ADMET properties (Table 4). The general evaluation in ADMET, absorption properties such as water (log mol/L) and intestinal solubility (% absorbed) and skin permeability (logKp) values justified the strong therapeutic potential of lead compounds. Literature study showed that compounds with good absorption results have more potency to cross gut barrier by passive penetration to reach the target molecule [33]. The water solubility results justified that compounds **4a-j** showed good absorption prediction. All compounds (**4a-j**) displayed good intestinal solubility results compared to standard value in literature (> 30%abs) [33]. Literature study showed that a compound with less than 30% absorbance value is considered as poorly absorbed compound [34]. The skin permeability values of all compounds were

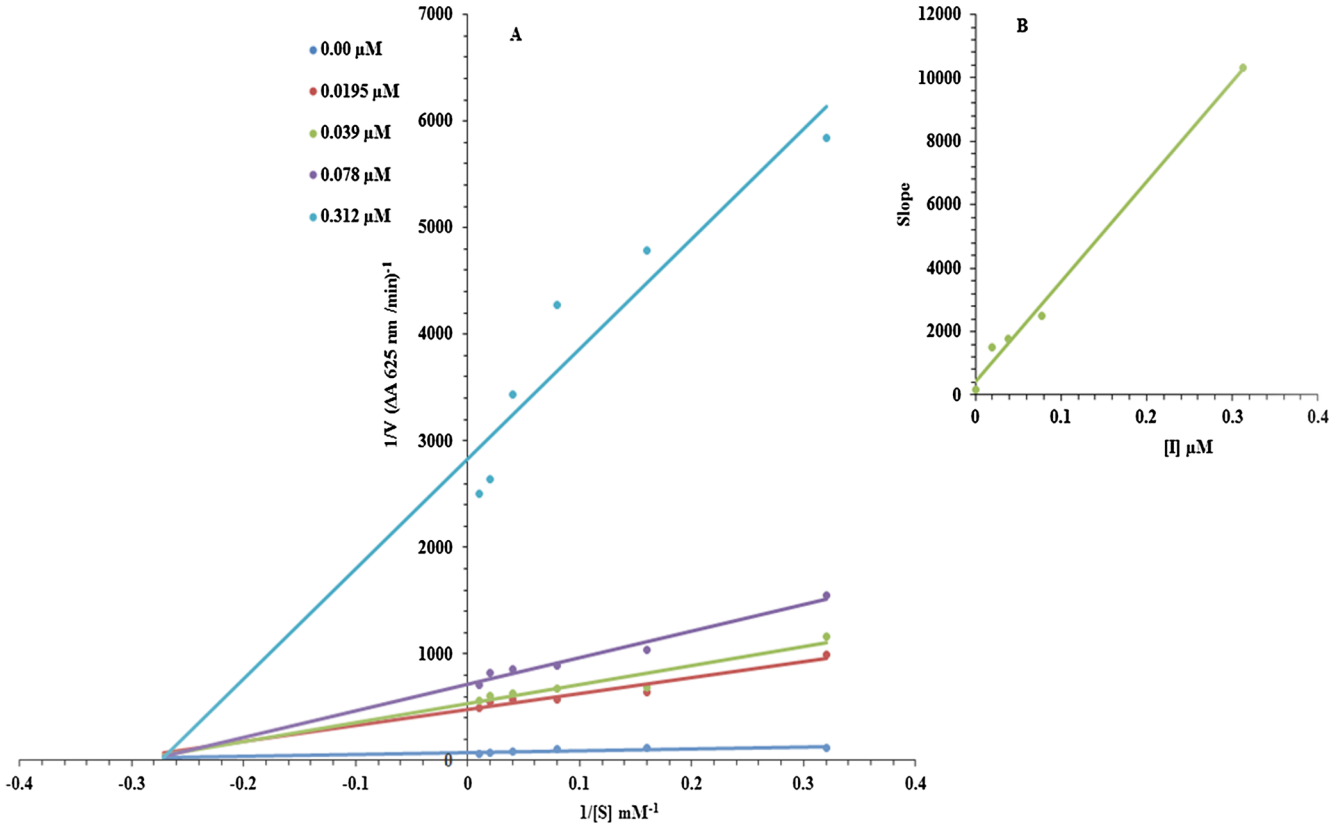

Fig. 2. Lineweaver–Burk plots for inhibition of Urease in the presence of inhibitor H1. (A) Concentrations of 4a were 0.00, 0.0195, 0.039, 0.078 and 0.312 µM. (B) The insets represent the plot of the slope or the vertical versus inhibitor 4a concentrations to determine inhibition constants. The lines were drawn using linear least squares fit.

also greater than standard value (−2.5 logKp) which showed their significance as a good lead structures and their drug likeness behavior. Moreover, blood brain barrier (BBB) and central nervous system (CNS) permeability values of all screened compounds were also comparable with the standard values (> 0.3 to < −1 log BB and > −2 to < −3 logPS) respectively. It has been observed that compounds with greater

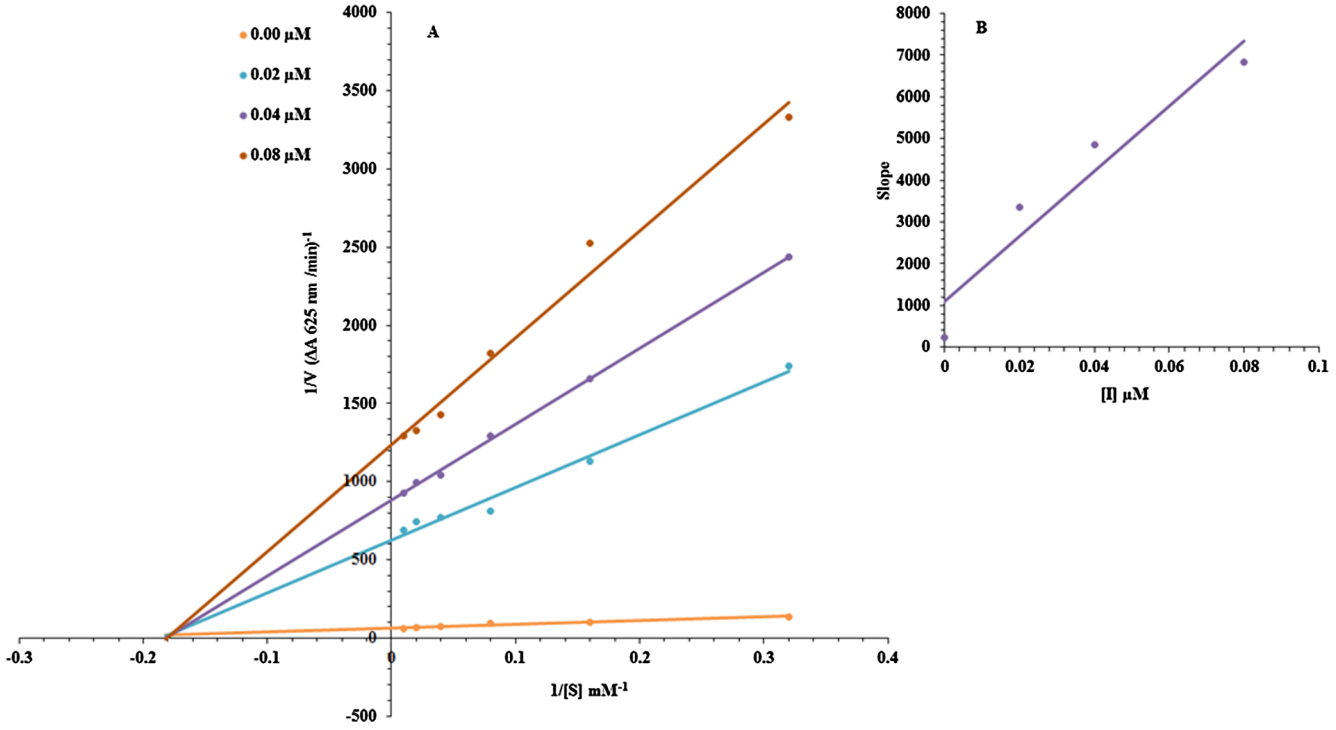

Fig. 3. Lineweaver–Burk plots for inhibition of Urease in the presence of inhibitor H1. (A) Concentrations of 4c were 0.00, 0.020.004, and 0.08 µM. (B) The insets represent the plot of the slope or the vertical versus inhibitor 4c concentrations to determine inhibition constants. The lines were drawn using linear least squares fit.

Table 2
Kinetic parameters of the jack bean urease for urea activity in the presence of different concentration of **4a** and **4c.**

Code	Dose (μM)	V_{max} (ΔA /Min)	K_m (mM)	Inhibition Type	K_i (μM)
	0.00	0.0151	3.546		
4a	0.0195	0.002	3.546	Non-Competitive	0.015
	0.039	0.0017	3.546		
	0.078	0.0014	3.546		
	0.312	0.0004	3.546		
	0.00	0.0168	5.208		
4c	0.02	0.00145	5.208	Non-Competitive	0.0145
	0.04	0.00108	5.208		
	0.08	0.00077	5.208		

V_{max} is the reaction velocity, Km is the Michaelis-Menten constant, Ki is the EI dissociation constant.

than 0.3 log BB value have potential to cross BBB, while with less than −1 value are poor distributed to brain. Similarly, the compounds have > −2 logPS value are considered to penetrate the CNS, while with < −3 are difficult to move in the CNS. Results showed that compounds displayed a significant potential to cross the barriers and may be target directly to receptor molecule. Moreover, their computational metabolic behavior was confirmed by CYP3A4, which is isoform of cytochrome P450 [35]. The excretion and toxicity predicted values were also justified the drug likeness behavior of these compounds on the basis of total clearance (log ml/min/kg), AMES toxicity, maximum tolerated dose (MTD) and LD_{50} values. The non-mutagenic and non-toxic behavior was also observed from AMES toxicity prediction. The hepatotoxicity negative behavior also showed their non-toxic and less sensitive effects. No compounds showed hepatotoxic behavior while most of compounds were depicts skin sensitive behavior except **4a, 4h** and **4i**. Skin sensitization character was also observed among all compounds and predicted results showed their negative behavior in the skin sensitization induction. These predicted ADMET properties results justified that these novel synthesized compounds showed good lead like potential for further evaluation.

4.6. Molecular docking analysis

4.6.1. Docking energy evaluation of synthesized compounds

To predict the best fitted conformational position within the active region of target protein all the synthesized compounds (**4a-j**) were docked against urease. The generated docked complexes were examined on the basis of minimum energy values (kcal/mol) and bonding interaction pattern. Docking results justified that compound **4a**, **4c**, **4f**, **4h** and **4i** exhibited a good binding energy values (-7.0, −7.1, −7.2, −7.0, and −7.0 kcal/mol), respectively compared to others compounds. The standard error for Autodock is reported as 2.5 kcal/mol [36]. However, compounds have no large docking energy value difference more than standard value. Since the basic nucleus of all the synthesized compounds were similar, most of ligands possess efficient energy values and have no significant energy fluctuations. The comparative binding energy analysis reveals that **4c** and **4f** was most active compound (Fig. 4). Our computational docking analysis also showed a good association with in-vitro study.

4.6.2. Binding pocket analysis of urease docked complexes

The docked complexes were further analyzed on the basis of binding interactions. However, the best conformational pose and energy valued docked complex (**4c**) is illustrated in Fig. 5. In detail, the structure activity relationship (SAR) study showed that four hydrogen bonds were observed in **4c** docked complex. The amino group of carbonyl chain is directly form hydrogen bond with His593 having bonding distance 3.15 Å. Whereas, oxygen group of benzene ring also form hydrogen bond with Met637 with bonding distances 2.12 Å, respectively. Similarly, carbonyl oxygen interacts with His519 and Asp494 by hydrogen interactions with binding distance 2.98 Å and 2.59 Å,

Table 3
Chemo-informatic properties of ligands.

Properties	4a	4b	4c	4d	4e	4f	4g	4h	4i	4j
MW	356.12	332.05	342.04	310.12	298.09	306.18	310.12	360.03	437.94	264.13
HBA	6	2	2	4	2	2	4	2	2	2
HBD	4	2	2	3	2	2	3	2	2	2
Log*P*	2.84	4.96	4.62	3.36	4.36	4.73	3.36	4.77	5.50	3.77
PSA (A^2)	108	32.60	33.30	71.56	32.60	31.90	71.56	32.60	31.90	33.30
Mol Vol.(A^3)	342.5	312.99	302.79	311.21	297.33	343.73	311.14	308.81	331.37	280.94
Drug Score	−1.55	0.10	−0.15	−1.17	−0.30	−0.18	−0.86	−0.70	−0.16	−0.69
RO5	Yes	Yes	Yes	Yes	Yes	Yes	Yes	Yes	No	Yes

Table 4
Pharmacokinetic assessment of synthesized compounds.

ADMET Properties		4a	4b	4c	4d	4e	4f	4g	4h	4i	4j
Absorption	WS (log mol/L)	−4.52	−4.59	−4.40	−4.09	−3.59	−4.26	−4.08	−4.50	−4.30	−3.29
	IS(%abs)	78.3	86.9	88.2	87.1	87.7	89.7	85.4	88.6	86.7	89.5
	SP(log Kp)	−2.7	−2.7	−2.7	−2.7	−2.7	−2.7	−2.7	−3.0	−2.9	−2.7
Distribution	BBBP (Log BB)	−0.81	0.03	0.07	−0.43	0.13	−0.04	−0.41	−0.07	−0.09	0.004
	CNSP (LogPS)	−2.89	−1.15	−1.37	−2.64	−1.49	−1.35	−2.64	−1.46	−1.64	−1.14
Metabolism	CYP3A4 inhibitor	Yes	Yes	No	Yes	Yes	No	Yes	No	Yes	Yes
Excretion	TC (log ml/min/kg)	0.20	0.19	−0.15	0.08	0.13	−0.14	0.01	−0.04	−0.3	−0.005
Toxicity	AMES toxicity	Yes	No	No	Yes	No	No	Yes	No	No	No
	Max. dose	−0.46	0.24	0.52	−0.04	0.41	0.46	0.02	0.55	0.79	0.18
	ORAT(LD_{50})	2.83	2.69	2.68	2.76	2.68	2.42	2.80	2.69	2.74	2.23
	HT	No	No	No	No	No	No	No	No	No	No
	SS	No	Yes	Yes	Yes	Yes	Yes	Yes	No	No	Yes

*Abbrevation: WS = Water solubility, IS = intestinal solubility, SP = skin permeability, BBBP = blood brain barrier permeability, CNSP = CNS permeability, TC = Total clearance, ORAT = Oral Rat Acute Toxicity, HT = Hepatotoxicity, SS = Skin Sensitization.

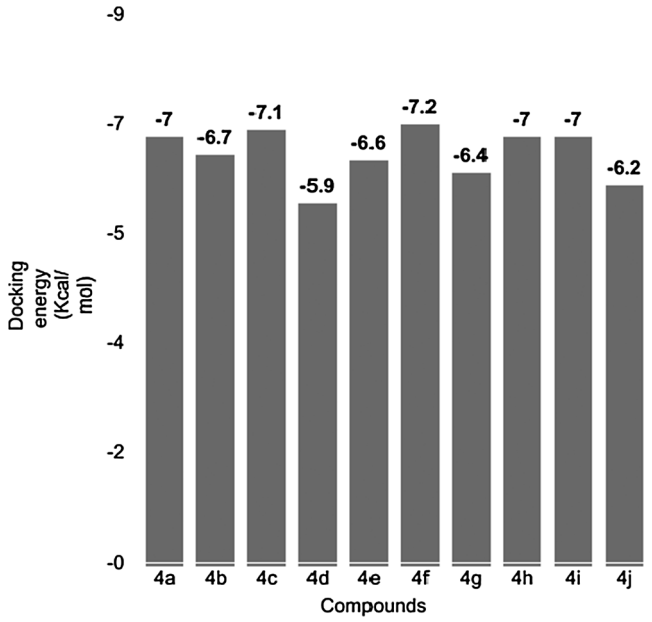

Fig. 4. The graphical depiction of docking energy values.

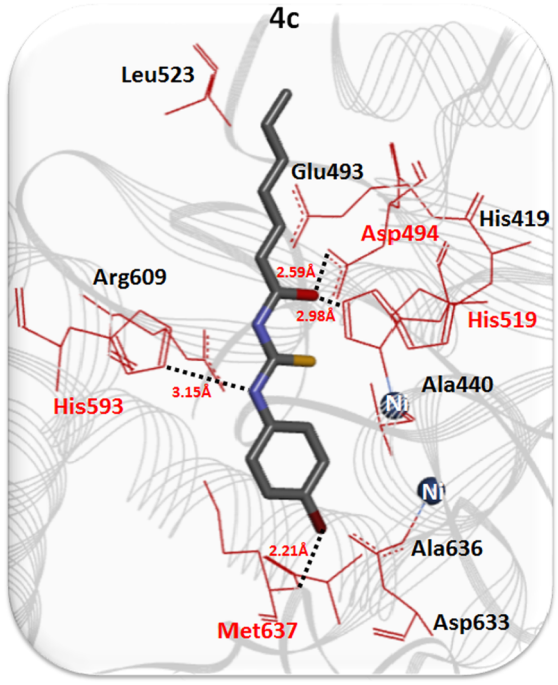

Fig. 5. Docking complex of **4c.** The ligand structure is displayed in grey color, while the functional groups such as amino, sulfur and oxygen are highlighted in light blue, yellow and red colors, respectively. The protein interacted amino acids are mentioned in maroon color in wire format. Two nickel atoms are also present. The black dotted lines represent the hydrogen binding and bond distances measured in angstrom (Å).

respectively. Literature data also ensured the importance of these residues in bonding with other urease inhibitors which strengthen our docking results [37]. The comparative binding energy and SAR analysis showed the significance of **4e** compound and may consider as potent inhibitors by targeting jack bean urease.

5. Conclusions

A new family of 1-heptanoyl-3-arylthioureas (**4a-4j**) was synthesized in straightforward way in excellent yield. The compounds were evaluated for Jack bean urease inhibition. All the compounds showed excellent activity against urease inhibition. The most potent derivative was **4a** containing two nitro group at *ortho* and *para* positions while the other potent derivative **4c** bore bromine at *para* position. The kinetic studies were performed to undermine the mode of inhibition of enzyme. Both derivatives were found to be non-competitive inhibitors. The K_i values for **4a** and **4c** were found to be 0.015 μM and 0.0145 μM. The chemo-informatics also revealed that these low-molecular weight target molecules can be used in drug designing. From the results of biological activity, kinetics and molecular docking it can be inferred that these molecules serve as structural templates for the designing potent drugs against Jack bean urease enzyme.

Acknowledgment

Supported by University Hospital in Hradec Kralove (No. 00179906).

Disclosure Statement

No potential conflict of interest was reported by authors.

Appendix A. Supplementary material

Supplementary data to this article can be found online at https://doi.org/10.1016/j.bioorg.2019.02.011.

References

[1] B. Zerner, Recent advances in the chemistry of an old enzyme, urease, Bioorg. Chem. 19 (1991) 116–131.
[2] M.J. Domínguez, C. Sanmartín, M. Font, J.A. Palop, S. San Francisco, O. Urrutia, F. Houdusse, J.M. García-Mina, Design, synthesis, and biological evaluation of phosphoramide derivatives as urease inhibitors, J. Agric. Food Chem. 56 (2008) 3721–3731.
[3] K.M. Khan, S. Iqbal, M.A. Lodhi, G.M. Maharvi, M.I. Choudhary, S. Perveen, Biscoumarin: new class of urease inhibitors; economical synthesis and activity, Bioorg. Med. Chem. 12 (2004) 1963–1968.
[4] F.A. Larik, A. Saeed, M. Faisal, P.A. Channar, S.S. Azam, H. Ismail, E. Dilshad, B. Mirza, Synthesis, molecular docking and comparative efficacy of various alkyl/aryl thioureas as antibacterial, antifungal and α-amylase inhibitors, Comput. Biol. Chem. 77 (2018) 193–198.
[5] S. Liu, B. Zhou, H. Yang, Y. He, Z.-X. Jiang, S. Kumar, L. Wu, Z.-Y. Zhang, Aryl vinyl sulfonates and sulfones as active site-directed and mechanism-based probes for protein tyrosine phosphatases, J. Am. Chem. Soc. 130 (2008) 8251–8260.
[6] R.L. Blakeley, J.A. Hinds, H.E. Kunze, E.C. Webb, B. Zerner, Jack bean urease (EC 3.5. 1.5). Demonstration of a carbamoyl-transfer reaction and inhibition by hydroxamic acids, Biochemistry 8 (1969) 1991–2000.
[7] W.S. Faraci, B.V. Yang, D. O'Rourke, R.W. Spencer, Inhibition of Helicobacter pylori urease by phenyl phosphorodiamidates: mechanism of action, Bioorg. Med. Chem. 3 (1995) 605–610.
[8] M. Şenel, A. Coşkun, M.F. Abasıyanık, A. Bozkurt, Immobilization of urease in poly (1-vinyl imidazole)/poly (acrylic acid) network, Chem. Pap. 64 (2010) 1–7.
[9] H.R. Allcock, S.R. Pucher, K.B. Visscher, Activity of urea amidohydrolase immobilized within poly [di (methoxyethoxyethoxy) phosphazene] hydrogels, Biomaterials 15 (1994) 502–506.
[10] P. Kosikowska, Ł. Berlicki, Urease inhibitors as potential drugs for gastric and urinary tract infections: a patent review, Expert Opin. Ther. Pat. 21 (2011) 945–957.
[11] Z. Amtul, R.A. Siddiqui, M.I. Choudhary, Chemistry and mechanism of urease inhibition, Curr. Med. Chem. 9 (2002) 1323–1348.
[12] A. Saeed, U. Flörke, M.F. Erben, A review on the chemistry, coordination, structure and biological properties of 1-(acyl/aroyl)-3-(substituted) thioureas, J. Sulfur Chem. 35 (2014) 318–355.
[13] J.D. Bloom, M.J. DiGrandi, R.G. Dushin, K.J. Curran, A.A. Ross, E.B. Norton, E. Terefenko, T.R. Jones, B. Feld, S.A. Lang, Thiourea inhibitors of herpes viruses. Part 1: bis-(aryl) thiourea inhibitors of CMV, Bioorg. Med. Chem. Lett. 13 (2003) 2929–2932.
[14] D.C. Schroeder, Thioureas, Chem. Rev. 55 (1955) 181–228.
[15] J. Wu, Q. Shi, Z. Chen, M. He, L. Jin, D. Hu, Synthesis and bioactivity of pyrazole acyl thiourea derivatives, Molecules 17 (2012) 5139–5150.
[16] F.A. Larik, A. Saeed, P.A. Channar, H. Ismail, E. Dilshad, B. Mirza, New 1-octanoyl-3-aryl thiourea derivatives: solvent-free synthesis, characterization and multi-target biological activities, Bangladesh J. Pharmacol. 11 (2016) 894–902.
[17] P.C. Nair, M.E. Sobhia, Quantitative structure activity relationship studies on thiourea analogues as influenza virus neuraminidase inhibitors, Eur. J. Med. Chem.

43 (2008) 293–299.
[18] J. Porter, Small molecule c-Met kinase inhibitors: a review of recent patents, Expert Opin. Ther. Pat. 20 (2010) 159–177.
[19] I. Koca, A. Özgür, K.A. Coşkun, Y. Tutar, Synthesis and anticancer activity of acyl thioureas bearing pyrazole moiety, Bioorg. Med. Chem. 21 (2013) 3859–3865.
[20] T. Schirmeister, U. Kaeppler, Non-peptidic inhibitors of cysteine proteases, Mini Rev. Med. Chem. 3 (2003) 361–373.
[21] Q. Zhang, X. Tang, F. Hou, J. Yang, Z. Xie, Z. Cheng, Fluorimetric urease inhibition assay on a multilayer microfluidic chip with immunoaffinity immobilized enzyme reactors, Anal. Biochem. 441 (2013) 51–57.
[22] I. Parejo, C. Codina, C. Petrakis, P. Kefalas, Evaluation of scavenging activity assessed by Co (II)/EDTA-induced luminol chemiluminescence and DPPH·(2, 2-diphenyl-1-picrylhydrazyl) free radical assay, J. Pharmacol. Toxicol. Method 44 (2000) 507–512.
[23] M. Faisal, F.A. Larik, A. Saeed, A highly promising approach for the one-pot synthesis of biscoumarins using HY zeolite as recyclable and green catalyst, J. Porous Mater. (2018), https://doi.org/10.1007/s10934-018-0625-0.
[24] E.F. Pettersen, T.D. Goddard, C.C. Huang, G.S. Couch, D.M. Greenblatt, E.C. Meng, T.E. Ferrin, UCSF chimera—a visualization system for exploratory research and analysis, J. Comput. Chem. 25 (2004) 1605–1612.
[25] E. Gasteiger, C. Hoogland, A. Gattiker, M.R. Wilkins, R.D. Appel, A. Bairoch, Protein identification and analysis tools on the ExPASy server, Proteomics Protoc. Handb., Springer, 2005, pp. 571–607.
[26] D. Studio, Discovery."version 2.1.," Accelrys San Diego, CA; 2008.
[27] L. Willard, A. Ranjan, H. Zhang, H. Monzavi, R.F. Boyko, B.D. Sykes, D.S. Wishart, VADAR: a web server for quantitative evaluation of protein structure quality, Nucleic Acids Res. 31 (2003) 3316–3319.
[28] L. Du, Z. Zhang, X. Luo, K. Chen, X. Shen, H. Jiang, Binding investigation of human 5-lipoxygenase with its inhibitors by SPR technology correlating with molecular docking simulation, J. Biochem. 139 (2006) 715–723.
[29] M. Faisal, S. Hussain, A. Haider, A. Saeed, F.A. Larik, Assessing the effectiveness of oxidative approaches for the synthesis of aldehydes and ketones from oxidation of iodomethyl group, Chem. Pap. 1–15 (2018).
[30] R.U. Kadam, N. Roy, Recent trends in drug-likeness prediction: A comprehensive review of In silico methods, Indian J. Pharm. Sci. 69 (2007) 609.
[31] P.A. Nogara, R.de A. Saraiva, D. Caeran Bueno, L.J. Lissner, C. Lenz Dalla Corte, M.M. Braga, D.B. Rosemberg, J.B.T. Rocha, Virtual screening of acetylcholinesterase inhibitors using the Lipinski's rule of five and zinc databank, Biomed. Res. Int. 2015 (2015).
[32] S. Tian, J. Wang, Y. Li, D. Li, L. Xu, T. Hou, The application of in silico drug-likeness predictions in pharmaceutical research, Adv. Drug Deliv. Rev. 86 (2015) 2–10.
[33] H.E. Selick, A.P. Beresford, M.H. Tarbit, The emerging importance of predictive ADME simulation in drug discovery, Drug Discov. Today 7 (2002) 109–116.
[34] A.R. Pries, L. Badimon, R. Bugiardini, P.G. Camici, M. Dorobantu, D.J. Duncker, J. Escaned, A. Koller, J.J. Piek, C. De Wit, Coronary vascular regulation, remodelling, and collateralization: mechanisms and clinical implications on behalf of the working group on coronary pathophysiology and microcirculation, Eur. Heart J. 36 (2015) 3134–3146.
[35] M. Faisal, A. Saeed, F.A. Larik, S.A. Ghumro, S. Rasheed, P.A. Channar, WOWS sol-gel based synthesis and structural, morphological, electrical and magnetic characterization of Co-Sm doped M-type barium hexaferrite materials, J. Electron. Mater. 47 (2018) 7011–7022.
[36] Z. Bikadi, E. Hazai, Application of the PM6 semi-empirical method to modeling proteins enhances docking accuracy of AutoDock, J. Cheminform. 1 (2009) 15.
[37] A. Hameed, K.M. Khan, S.T. Zehra, R. Ahmed, Z. Shafiq, S.M. Bakht, M. Yaqub, M. Hussain, A. de la, V. de León, N. Furtmann, Synthesis, biological evaluation and molecular docking of N-phenyl thiosemicarbazones as urease inhibitors, Bioorg. Chem. 61 (2015) 51–57.